

# Reactive and Nonreactive Fluorescent Probes for Monitoring the Photoinitiated Polymerization of Dimethacrylates: The Role of Luminophore Distribution in Heterogeneous Environments

Wolter F. Jager\* and Ben Norder

Department of Polymer Materials and Polymer Engineering, Delft University of Technology, Julianalaan 136, 2628 BL Delft, The Netherlands

Received April 26, 2000; Revised Manuscript Received September 6, 2000

**ABSTRACT:** Reactive (**2**, **4**) and corresponding nonreactive (**3**, **5**) fluorescent probes, based on 4-(dimethylamino)-4'-nitrostilbene (**1**), have been employed for monitoring the photoinitiated polymerization of a series of dimethacrylates. Reactive fluorescent probes are significantly more sensitive, in particular at the early stages of the polymerization process. The observed differences in emission between reactive and nonreactive probes can be explained by assuming that covalent attachment affects the distribution of probe molecules between rigid environments, presumably highly cross-linked gel particles, and mobile monomer-rich environments. Enrichment of nonreactive probes in mobile environments is expected due to diffusion out of the cross-linking regions.

## Introduction

Photoinitiated polymerizations are frequently employed as a means of producing highly cross-linked polymers for abrasion resistant coatings, optical fibers, microelectronic devices, and dental restorative materials.<sup>1,2</sup> Since light initiates the polymerization and solventless formulations are employed, the process consumes little energy and emission of volatile organic compounds does not occur. Most formulations contain a large fraction of multifunctional monomers since cross-linked networks are required for most applications and addition of multifunctional monomers strongly increases the rate of polymerization.

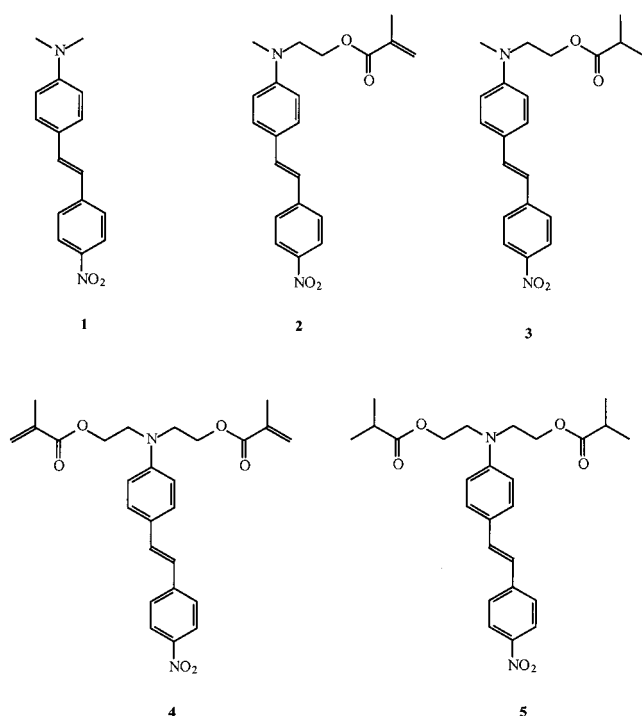
The polymerization of di(meth)acrylates is a process that forms highly inhomogeneous networks, and detailed information concerning structure formation during these processes is available from a number of studies.<sup>3–5</sup> The formation of microgels<sup>6</sup> during the initial stages of the thermal polymerization of ethylene glycol dimethacrylate (EGDMA) was investigated using light scattering techniques.<sup>3</sup> Microgel particles were observed right from the beginning of the reaction, even at conversions below 1%. Up to macroscopic gelation, around 15% conversion, the amount and size of the microgel particles increased along with the pendant double-bond conversions within the particles.<sup>7</sup> A bimodal size distribution was observed in small particles that are 15–20 nm in diameter and larger structures that are approximately 50–100 nm in diameter. Transmission electron microscopy on OsO<sub>4</sub>-stained films obtained from the photoinitiated polymerization of triethylene glycol dimethacrylate (TREGDMA) revealed the highly inhomogeneous nature of the photoformed polymer after gelation.<sup>4</sup> Two types of polymer-rich regions were observed: 50–100 nm in diameter and approximately 10 nm in diameter. These are the remnants of microgel particles that were formed before macroscopic gelation. Extraction experiments performed during the photoinitiated polymerization of hexanedioldiacrylate (HDDA) have determined the fraction of pendant double bonds in the photoformed polymer.<sup>5</sup> During the first stage of the reaction a strong increase in pendant double-bond

conversion was observed, and this might be the stage of the reaction before macroscopic gelation where individual microgel particles are growing. During a second stage in the reaction, 10–80% relative conversion, the fraction of pendant double bonds in the polymer remains constant. This implies that the cross-link density in the polymer phase is constant,<sup>8</sup> and most likely microgel particles grow together in this stage of the reaction. During the last stages of the polymerization the conversion of pendant double bonds in the polymer fraction increases once more, and highly cross-linked networks are formed.

In contrast to linear, soluble polymers, the characterization of polymer networks requires special techniques capable of handling solid samples. Monomer conversion and final properties such as cross-link density, mechanical properties, surface morphology, and free volume are determined by a number of mechanical, microscopic, and spectroscopic techniques.<sup>9</sup> The physical properties of photoformed networks are not determined by the formulation of the reactants *exclusively*, but to a large extent also by the exact method of preparation and the resulting rate of polymerization. In the case of photoinitiated polymerization processes the rate of polymerization is governed by the concentration of photoinitiator and the light intensity. Therefore, polymerization processes are often monitored in real time for obtaining complementary information about structure formation.<sup>2</sup> Well-known techniques for real time monitoring of photoinitiated polymerization reactions are FT-IR spectroscopy,<sup>10</sup> absorption spectroscopy,<sup>11</sup> photo-DSC,<sup>12</sup> and fluorescence spectroscopy, using either inherent fluorescence<sup>13</sup> or emission from added fluorescent probes.

For monitoring photoinitiated polymerization reactions various fluorescent probes have been developed over the years. During a polymerization process, the anisotropy, the wavelength  $\lambda_{\text{max}}$ , the intensity  $I_{\text{max}}$ , and the half-width of emission may change. Monitoring the position of probe emission is the preferred method in many cases, since this is very sensitive, is easily automated,<sup>14</sup> and can be applied for samples of various

Scheme 1. Probes 1–5



sizes and shapes. Examples of fluorescent probes whose emission wavelengths shift to the blue during polymerization processes are excimer-forming probes,<sup>15</sup> intramolecular charge transfer probes,<sup>16</sup> intramolecular twisted charge-transfer probes,<sup>17</sup> and organic salts of the  $D-\pi-A^+X^-$  type.<sup>18</sup>

Until this time, most experiments using fluorescent probes for monitoring photoinitiated polymerization processes have been carried out with nonreactive luminophores like **1**.<sup>19</sup> By attaching reactive groups to the luminophore, fundamental changes can be expected in the interactions between a probe and the surrounding matrix. Nonreactive probes like **1**, **3**, and **5** (Scheme 1) dissolve in the monomer as well as in the photoformed polymer and are free to migrate within the constraints of the polymerizing medium. In dimethacrylates, which form inhomogeneous networks with large variations in cross-link density throughout the polymerization process,<sup>3</sup> diffusion of probe molecules out of cross-linking regions is expected.<sup>20</sup> Therefore, nonreactive probe molecules will be accumulated in monomer-rich, mobile environments. Reactive probes,<sup>21</sup> like **2** and **4**, in which one or two methacrylate moieties are attached to the luminophore, interact with their direct environment in a fundamentally different fashion. The probe dissolved in monomer will become covalently attached to the polymer backbone during the polymerization process. It is expected that, due to their immobilization during the polymerization process, reactive probes will be distributed more evenly throughout the medium. A faster incorporation in the rigid polymer network is expected for the dimethacrylate **4** compared to the monomethacrylate **2**.<sup>20,22</sup> As the medium is highly heterogeneous and shifts in emission between probes in monomer-rich and fully polymerized regions readily exceeds 100 nm for the DMANS luminophore,<sup>16a</sup> changes in the probe distribution must have a serious impact on the overall emission of the probe.

The purpose of the work reported is to describe the fluorescence of **1**–**5** during the photoinitiated polymer-

ization of a series of dimethacrylates. In particular, the performance of reactive probes in comparison to *corresponding* nonreactive probes, i.e., the effect of attaching probe to the polymer backbone, has been investigated. Taking EGDMA as a typical monomer, the results obtained here are compared with those obtained previously with MMA.<sup>23</sup> The striking differences observed are discussed, and a general mechanism explaining the emission of **1**–**5** during the polymerization of dimethacrylates will be proposed.

## Experimental Section

**General.** The dimethacrylates ethylene glycol dimethacrylate (EGDMA), diethylene glycol dimethacrylate (DEGDMA), triethylene glycol dimethacrylate (TREGDMA), tetraethylene glycol dimethacrylate (TEEGDMA), butanediol dimethacrylate (BUDMA), and hexanediol dimethacrylate (HEXDMA) were purchased from Aldrich and used as received. Irgacure 907 (2-methyl-1-[4-(methylthio)phenyl]-2-morpholinopropanone-1) was a gift from Ciba-Geigy. The fluorescent probes (**1**–**5** and **P2**)<sup>24</sup> were synthesized as recorded previously.<sup>23</sup>

Extraction experiments were performed by placing freshly prepared, 75  $\mu\text{m}$  thick samples (irradiation time 20 min, [probe] =  $10^{-3}$  mol kg<sup>-1</sup>) in 10 mL of acetone or 2-butanone in small sealed vials at 50 °C.

**Spectroscopic Measurements.** Fluorescence measurements were recorded on a PTI Quantamaster spectrofluorimeter at right angles, using 420 nm as the excitation wavelength. Spectra were analyzed using the software package Table Curve (Jandel). Absorption spectra were recorded on a Contron Instruments spectrophotometer, and IR spectra were measured on a Mattson 6020 Galaxy series FT-IR spectrometer. Photo-DSC measurements were recorded on a modified Perkin-Elmer DSC 7 apparatus. The modification consists of two quartz-covered holes in the lid above which a Philips PL-S 9W/10 low-pressure mercury lamp was mounted.

**Photoinitiated Polymerizations.** Polymerization was achieved by exposing films to UV radiation from a Philips PL-S 9W/10 low-pressure mercury lamp for successive periods of time. Besides the typical mercury lines in the visible, the emission of this lamp has a broad emission around 365 nm (ca. 2 mW/cm<sup>2</sup>, HW  $\approx$  17 nm). After each irradiation period films were analyzed by fluorescence or FT-IR spectroscopy. Irgacure 907 (1 wt %) was used as the photoinitiator, and fluorescent probes, typically  $1.0 \times 10^{-4}$  mol kg<sup>-1</sup>, were added. Films were made by squeezing a drop of monomer between microscope slides divided by 75  $\mu\text{m}$  polypropylene spacers. A metal holder with 30  $\times$  10 mm windows was used. Double-bond conversions were determined for 15  $\mu\text{m}$  films between NaCl plates by FT-IR, using the typical methacrylate absorption at 817 cm<sup>-1</sup>. The CH stretch vibrations at 3200–2800 cm<sup>-1</sup> were used as a reference signal to compensate for differences in sample thickness. The double-bond conversions of a dimethacrylate as a function of the irradiation time between glass plates were calculated by employing a correlation between the cure of the dimethacrylate and  $\lambda_{\text{max}}$ .

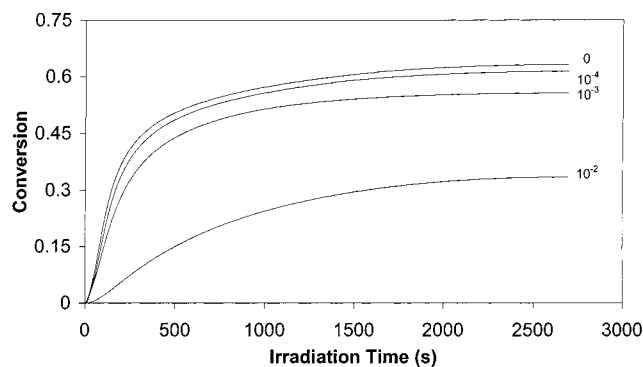
## Results

The synthesis and physical characterization of **1**–**5** and **P2**<sup>24</sup> were reported previously.<sup>23</sup> Attaching larger moieties to the amino group of the luminophore, including covalent attachment to a polymer, induces blue shifts in emission and increases in the quantum yields of fluorescence  $\Phi_f$ . The emission spectra of corresponding probes, bearing either methacrylates (**2** and **4**) or isobutryryl esters (**3** and **5**), however, are identical.

Reaction rates of photoinitiated polymerization for formulations with various probe concentrations were determined using photo-DSC. Selected results are displayed in Table 1 and Figure 1. For formulations without probe added the order of the rate of polymeri-

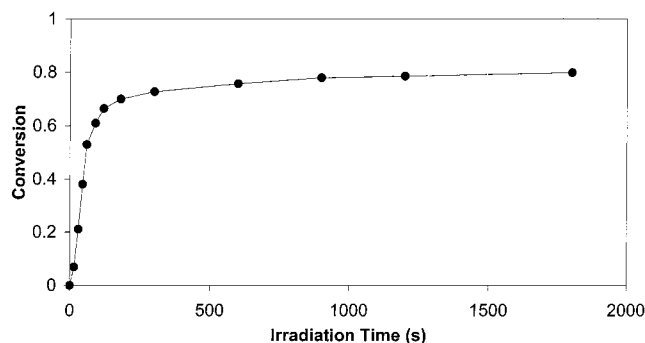
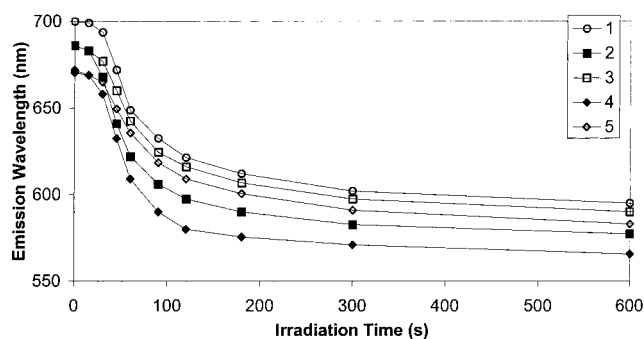
**Table 1. Photo-DSC Results for Formulations Using 2 as Added Fluorescent Probe**

resin	[PI] <sup>a</sup>	[2] <sup>b</sup>	final conv	max rate <sup>c</sup>	(conv)
EGDMA	1.0	0	0.63	$2.1 \times 10^{-3}$	(0.26)
EGDMA	1.0	$1 \times 10^{-4}$	0.61	$1.9 \times 10^{-3}$	(0.24)
EGDMA	1.0	$1 \times 10^{-3}$	0.57	$1.4 \times 10^{-3}$	(0.20)
EGDMA	1.0	$1 \times 10^{-2}$	>0.35 <sup>d</sup>	$2.5 \times 10^{-4}$	(0.12)
HEXDMA	1.0	0	0.75	$4.0 \times 10^{-3}$	(0.39)
HEXDMA	1.0	$1 \times 10^{-4}$	0.75	$4.0 \times 10^{-3}$	(0.39)
HEXDMA	1.0	$1 \times 10^{-3}$	0.72	$2.8 \times 10^{-3}$	(0.34)
HEXDMA	1.0	$1 \times 10^{-2}$	>0.39 <sup>d</sup>	$4.8 \times 10^{-4}$	(0.13)
TEEGDMA	1.0	0	0.89	$7.0 \times 10^{-3}$	(0.55)
TEEGDMA	1.0	$1 \times 10^{-4}$	0.89	$7.0 \times 10^{-3}$	(0.55)
TEEGDMA	1.0	$1 \times 10^{-3}$	0.88	$5.1 \times 10^{-3}$	(0.52)
TEEGDMA	1.0	$5 \times 10^{-3}$	0.84	$2.0 \times 10^{-3}$	(0.30)

<sup>a</sup> In wt %. <sup>b</sup> In mol kg<sup>-1</sup>. <sup>c</sup> Methacrylate disappearance in s<sup>-1</sup>.<sup>d</sup> Inaccurate due to slow reaction, final conversion not obtained.**Figure 1.** Photo-DSC exotherms for EGDMA formulations containing 1% photoinitiator without probe and with 2 at  $1.0 \times 10^{-4}$ ,  $1.0 \times 10^{-3}$ , and  $1.0 \times 10^{-2}$  mol kg<sup>-1</sup>.

zation is TEEGDMA > TREGDMA > DEGDMA ≈ HEXDMA > BUDMA > EGDMA. The rate of polymerization increases as the length of the spacer between the methacrylates increases. Not the concentration, but the mobility of methacrylates in dangling ends appears to be the major factor determining the reactivity of the monomers. Table 1 shows that rates of polymerization and final conversions were strongly reduced in all resins by adding  $10^{-2}$  mol kg<sup>-1</sup> probe. At [probe] =  $10^{-3}$  mol kg<sup>-1</sup>, final conversions were close to those obtained without addition of probe, but the rate of polymerization is reduced considerably. At a probe concentration of  $10^{-4}$  mol kg<sup>-1</sup> the rates of polymerization and the final conversions in TEEGDMA, TREGDMA, and HEXDMA are identical to those of formulations without added probe. In EGDMA, BUDMA, and DEGDMA slightly decreased values compared to those of formulations without added probe were observed. Figure 1 shows the conversion as a function of the reaction time for EGDMA formulations containing 2 at different concentrations. At all probe concentrations, it was found that final conversions and rates of polymerization were identical within experimental error for 1–5.

UV spectra reveal that competitive absorption is the major factor reducing the rate of polymerization. Since the absorption spectra of 1–5 are very similar, the proportion of light absorbed by the probes and the reductions in reaction rate due to competitive absorption are virtually identical for all probes. The addition of photoformed radicals to the probe molecules, a process that causes bleaching, will also retard the polymerization process. At low probe concentration, however, it has been demonstrated that the consumption of radicals by this pathway is negligible. It is concluded that at probe

**Figure 2.** Double-bond conversions as a function of the accumulated irradiation time for a standard EGDMA formulation ([PI] = 1%, [probe] =  $10^{-4}$  mol kg<sup>-1</sup>) as determined by FT-IR measurements.**Figure 3.** Emission wavelength  $\lambda_{\max}$  of 1–5 in EGDMA as a function of the irradiation time.

concentrations of  $10^{-4}$  mol kg<sup>-1</sup> the rates of the polymerization reaction were slightly reduced in dimethacrylates with short spacers only.

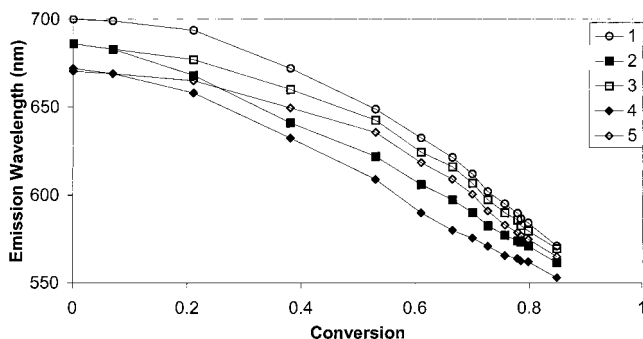
The double-bond conversion in EGDMA as a function of the accumulated irradiation time for formulations containing  $1.0 \times 10^{-4}$  mol kg<sup>-1</sup> probe was determined by FT-IR spectroscopy and displayed in Figure 2. For these experiments formulations are irradiated, an IR spectrum is taken, and subsequently the sample is irradiated again. At conversions between 45 and 70%, corresponding to irradiation times between 45 and 180 s, the dark reaction takes place at considerable rates, and one should be aware of this in order to obtain reproducible and reliable results.<sup>16b</sup>

Covalent attachment of reactive probes to the polymer network was proven by extraction experiments employing 2 and 3 in fully cured films. Probe 3 could be extracted, but the reactive probe 2 could not be extracted, as expected. The extent of probe extraction strongly depends on maze size of the networks. The amount of nonreactive probe extracted from poly-EGDMA is negligible, but as the length of the side chains in the network increases, more nonreactive probe could be extracted. Quantitative recovery of 3 was achieved only from poly-TEEGDMA films.

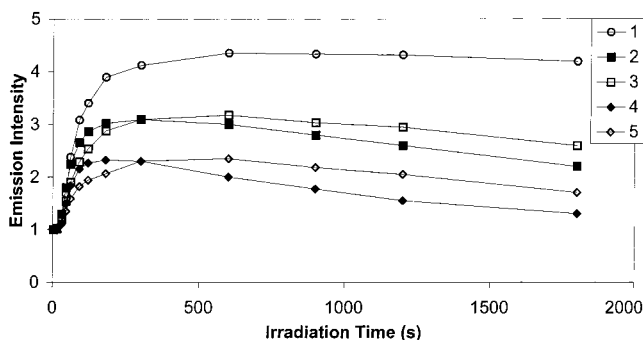
**Emission Spectra.** The emission wavelengths  $\lambda_{\max}$ , relative emission intensities  $I_{\max}$ , and the half-widths (HW) of the emissions of 1–5 in EGDMA as a function of accumulated irradiation times or double-bond conversions are displayed in Figures 3–6. The emission wavelengths  $\lambda_{\max}$  of 1–5 in various dimethacrylates before and after polymerization are displayed in Table 2.

Table 2 shows that all for all probe–resin combinations strong blue shifts in emission are observed upon polymerization. Comparing the nonreactive probes 1, 3,





**Figure 4.** Emission wavelength  $\lambda_{\max}$  of 1–5 in EGDMA as a function of the double-bond conversion.



**Figure 5.** Emission intensity  $I_{\max}$  of 1–5 in EGDMA as a function of the irradiation time.

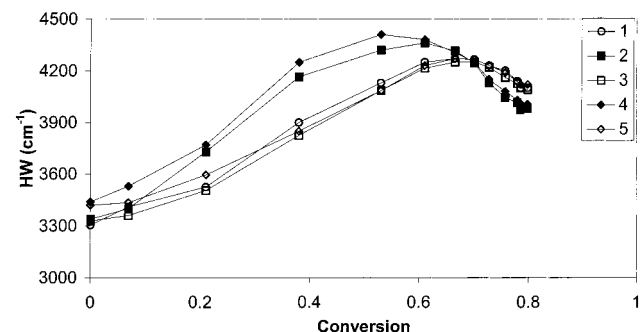


**Figure 6.** Half-widths of the emissions of 1–5 in EGDMA as a function of the double-bond conversion.

and 5, it is concluded that attaching larger groups to the amino nitrogen decreases the overall sensitivity<sup>25</sup> of the probes in the “apolar” resins EGDMA, BUDMA, and HEXDMA, typically by 150  $\text{cm}^{-1}$  per substituent. In the “polar” resins DEGDMA, TREGDMA, and TEEGDMA, on the other hand, the overall sensitivity is virtually identical for all nonreactive probes. By replacing an isobutyryl group with a methacryloyl group, i.e., converting a nonreactive probe into a reactive probe, the overall blue shift of the probe is *always* increased, irrespective of the resin structure, typically by 100–250  $\text{cm}^{-1}$  per substituent. The largest shifts, 250  $\text{cm}^{-1}$  per substituent, are observed in EGDMA, and shifts decrease as the length of the spacer between the methacrylate moieties in the monomer; i.e., the maze size in the network, increases. For all probe–resin combinations considerable blue shifts, typically 10 nm, are observed upon leaving sealed samples in the dark. These shifts, which can be increased by heating, are primarily due to aftercure, a process that is detected by FT-IR spectroscopy.

Figures 3 and 4 display the emission wavelength of 1–5 in EGDMA as a function of the irradiation time

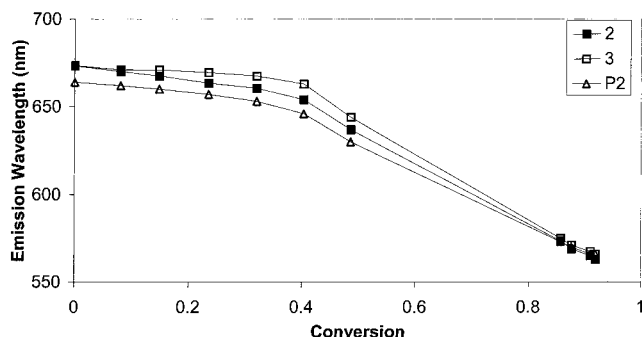
**Table 2. Emission Wavelengths  $\lambda_{\max}$  of 1–5 in Various Dimethacrylates before and after a 20 min Irradiation Procedure, along with the Observed Shifts in nm and  $\text{cm}^{-1}$**

		1	2	3	4	5
HEX	mon	676	662	662	649	649
	pol	568	560	563	553	559
	shift (nm)	108	102	99	96	90
	shift ( $\text{cm}^{-1}$ )	2815	2765	2655	2690	2495
BU	mon	688	672	672	660	660
	pol	578	566	573	558	568
	shift (nm)	110	106	99	102	92
	shift ( $\text{cm}^{-1}$ )	2770	2805	2585	2770	2455
EG	mon	701	686	686	672	672
	pol	585	571	580	562	575
	shift (nm)	116	115	106	110	97
	shift ( $\text{cm}^{-1}$ )	2840	2935	2680	2915	2510
DEG	mon	709	695	695	682	682
	pol	592	580	585	571	577
	shift (nm)	117	115	110	111	105
	shift ( $\text{cm}^{-1}$ )	2775	2870	2705	2850	2655
TREG	mon	711	698	698	682	682
	pol	603	590	596	578	585
	shift (nm)	108	108	102	104	97
	shift ( $\text{cm}^{-1}$ )	2505	2640	2450	2640	2430
TEEG	mon	709	699	699	684	684
	pol	616	602	606	588	598
	shift (nm)	93	97	93	96	86
	shift ( $\text{cm}^{-1}$ )	2130	2295	2185	2385	2115

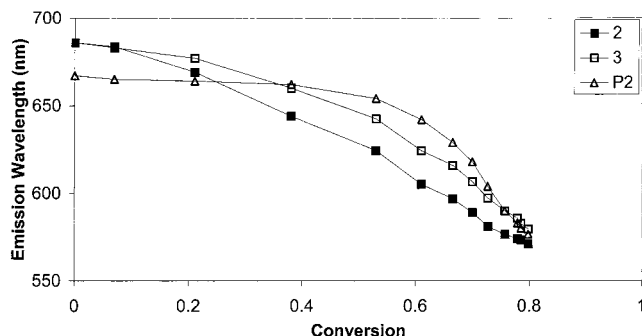
and the conversion, respectively. Throughout the reaction, reactive probes exhibit larger blue shifts in  $\lambda_{\max}$  than corresponding nonreactive probes. These differences strongly increase during the first stages of the reaction, reach a maximum, and gradually decrease later on. Comparing 2 and 3, differences in  $\lambda_{\max}$  values up to 20 nm are observed, while for 4 and 5 differences up to 30 nm are found. In all monomers differences in  $\lambda_{\max}$  values between corresponding reactive and nonreactive probes are larger for the difunctional probes 4 and 5 compared to the monofunctional probes 2 and 3.

Figure 4 shows the emission wavelength  $\lambda_{\max}$  of 1–5 in EGDMA as a function of the double-bond conversion. The beginning of the reaction, up to a 6% conversion, is not detected by any of the probes. At conversions above 20%, the emission wavelength decrease becomes almost linear with conversion for reactive probes. This implies that reactive probes are sensitive probes above a 20% conversion. For nonreactive probes the gradient increases slower, and a constant value is obtained above a 50% conversion. This means that nonreactive probes are particularly suited to monitor the reaction at high conversions. For polymer bound probes like P2,<sup>24</sup> the shift of  $\lambda_{\max}$  as a function of conversion is even more pronounced. This probe does not detect the polymerization process up to conversions of 40% but is extremely sensitive during the latter stages of the polymerization process at conversions above 70%; see Figure 8.

The normalized emission intensity of 1–5 as a function of the irradiation time is shown in Figure 5. The observed intensities are the result of two opposing effects: an increase in  $\Phi_f$  and a decrease in probe concentration as the reaction proceeds. The extent of probe degradation or bleaching<sup>26</sup> was determined by UV spectroscopy. For highly concentrated solutions ( $[\text{probe}] = 10^{-2} \text{ mol kg}^{-1}$ ) decreases of  $A_{\max}$  by 31, 24, 39, and 25% were observed for 2, 3, 4, and 5, respectively, after 40 min irradiation periods. These indicate a faster bleaching of the reactive probes. In addition, a more pronounced peak broadening that was observed



**Figure 7.** Emission wavelength  $\lambda_{\max}$  of **2**, **3**, and **P2** in MMA as a function of the double-bond conversion.



**Figure 8.** Emission wavelength  $\lambda_{\max}$  of **2**, **3**, and **P2** in EGDMA as a function of the double-bond conversion.

in the absorption spectra of reactive probes also contributes to the decreases in  $A_{\max}$ .

Figure 5 compares the emission intensities of **1–5** in  $10^{-4}$  mol kg $^{-1}$  formulations and shows that the emission intensities of reactive probes increase faster at the beginning of the polymerization. At the later stages of the reaction emission intensities decrease since the bleaching process exceeds the increases in  $\Phi_f$ . Markedly slower decreases in the emission intensities are observed for the nonreactive probes, resulting in higher emission intensities at the end of the reaction.

The steeper increase of  $I_{\max}$  for reactive probes is explained by a faster incorporation of the probes in a rigid network in which  $\Phi_f$  is a factor 4, 6, and 8 higher than in the monomer for **1**, **2/3**, and **4/5**, respectively.<sup>27</sup> At the later stages of the reaction a faster incorporation in rigid environments is expected for the nonreactive probes, hence the slower decrease in emission intensity. The slower decrease in emission intensity observed for nonreactive probes is further enhanced by a slower decrease in absorption, indicative of slower probe decomposition.

The width of the emission generally is an indication of the homogeneity of the medium in which the probe is incorporated. The data displayed in Figure 6 show significant differences in half-widths for reactive and nonreactive probes. For all probes, HW values increase, reach a maximum, and subsequently decrease at later stages of the reaction. These values indicate that the luminophores are present in distinct environments in a heterogeneous system. Faster rises in half-width and higher maxima are observed for reactive probes, indicating a faster incorporation in highly cross-linked regions. For all nonreactive probes the maximum values of HW are observed at a 70% conversion, while for the reactive probes the maximum values of HW are observed earlier at a 50–60% conversion. At final conversions lower half-widths are observed for reactive probes.

## Discussion

Significant differences in emission spectra between corresponding reactive and nonreactive probes are observed during the photoinitiated polymerization of dimethacrylates. In particular, during the first stages of the reaction, up to conversions of 50%, blue shifts of  $\lambda_{\max}$ , increases in  $I_{\max}$ , and HW are larger for reactive probes. Covalent attachment of reactive probes to the polymer backbone was proven by extraction experiments and *must be* the sole factor responsible for these differences. For describing the differences in emission between reactive and nonreactive probes observed during the photoinitiated polymerization, two mechanisms are proposed.<sup>28</sup>

The first mechanism assumes that covalent attachment to the polymer backbone is the only difference between reactive and nonreactive probes. Apart from this attachment, both types of probes are in exactly the same environment, and a steadily increasing concentration of polymer bound probe, a distinct luminescent species, causes the differences in emission between reactive and nonreactive probes. For the photoinitiated polymerization of MMA, a reaction that produces a fairly homogeneous medium, this mechanism describes the differences between reactive and nonreactive probes in a satisfactory manner, as is illustrated in Figure 7. In Figure 7  $\lambda_{\max}$  values of **2**, **3**, and **P2**, the polymer obtained by a copolymerization of **2** with MMA, are plotted as a function of the irradiation time. Emission wavelengths for **2** are *always* between those of **3** (identical to “free” **2**) and **P2** (identical to covalently attached **2**). Figure 7 shows that incorporation of **2** in the PMMA backbone results in blue shifts, whose magnitude depends on the conversion. The blue shift in MMA is 7 nm, and as the conversion increases, this value is increased to 15 nm at a 40% conversion. At higher conversions the differences between dissolved and attached probes decrease and virtually disappear at full conversion. The observation that the emission of **P2** and **3** become identical at higher conversions is not surprising since covalent attachment to the polymer backbone is not expected to alter the mobility of a luminophore in a glassy polymer matrix.

Figure 4 plots the  $\lambda_{\max}$  values of **2–5** in EGDMA as a function of the irradiation time. The large differences between the emission wavelengths of **2** and **3** suggest that differences between free and polymer bound probes should be on the order of 50 nm at 40% conversion. At higher conversions the differences between reactive and nonreactive probes decrease but do not disappear. Both observations suggest that covalent incorporation cannot be the main reason for the differences between reactive and nonreactive probes.

The alternative mechanism takes into account that during the photoinitiated polymerization of dimethacrylates inhomogeneous media are formed. Both reactive and nonreactive probes reside in various environments ranging from free monomer to fully cured networks. Observed emission spectra are the sum of the emissions of all luminophores and blue shifts are caused by changes in the distribution of luminophores over the various environments. As the reaction proceeds, the number of luminophores in mobile media decrease while those in rigid environments increase. Nonreactive probes are mobile throughout the reaction, will be expelled from densely cross-linked regions, and will become enriched in mobile environments. Reactive probes, on the other

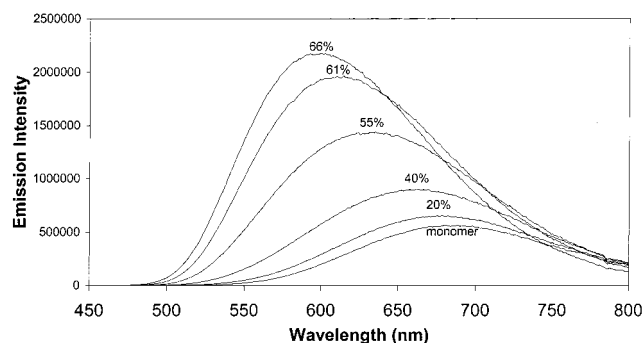


**Figure 9.** Emission spectra of **3** ( $10^{-2}$  mol kg $^{-1}$ ) in EGDMA at different double-bond conversions.

hand, are anchored to the polymer network and are expected to be more evenly distributed throughout the medium at all stages of the reaction. Since reactive probes are incorporated in rigid environments at higher rates, these are more sensitive, especially at the beginning of the reaction.

The data displayed in Figures 4, 6, and 8 are strongly in favor of the second mechanism. The large, nonvanishing differences in  $\lambda_{\text{max}}$  values between the reactive and nonreactive probes in Figure 4 are in accordance with this mechanism. The pronounced differences in HW values between the reactive and nonreactive probes displayed in Figure 6 indicate that the distribution of the luminophore over various environments is different for each type of probe. Covalent attachment can lead to some broadening, but as the emission wavelengths  $\lambda_{\text{max}}$  of bound and unbound probes are very similar, modest increases on the order of 100 cm $^{-1}$  are expected.<sup>29</sup> Reactive probes are expected to be incorporated in rigid environments at higher rates, thus causing a steeper increase in HW values. The earlier decrease in HW observed for reactive probes might be due a faster disappearance of luminophores in a mobile environment. As emissions from these mobile environments disappear, the probe emission indicates the formation of a more homogeneous rigid environment. The intriguing behavior of **P2** in EGDMA displayed in Figure 8 seems to indicate that the diffusion out of cross-linking regions is correlated to the dimensions of the fluorescent probe used. Up to a 55% conversion **P2** does not detect the polymerization, indicating that **P2** still resides in mobile environments. At higher conversions **P2** becomes highly sensitive, but both  $\lambda_{\text{max}}$  and HW values indicate that the luminophores in **P2** resides in an environment strongly resembling PMMA throughout the reaction. Most likely a phase separation between **P2** and poly-EGDMA takes place at high conversions.

From the previous discussion it is concluded that the mechanism that assumes difference in probe distribution for reactive and nonreactive in a heterogeneous environment is the most realistic. From this it follows that the distribution of luminophores over various environments is the key element in describing the emission of **1–5** in dimethacrylates. It should be noted that, according to this mechanism, differences in emission wavelengths for reactive and nonreactive probes are indicative for the heterogeneity of the network. Emission spectra of **3** as a function of the double-bond conversion are displayed in Figure 9.<sup>30</sup> From these spectra the emission characteristics in monomer and densely cross-linked networks can be derived. For **3** in EGDMA values for  $\lambda_{\text{max}}$ ,  $I_{\text{max}}$ , and HW obtained in

monomer and densely cross-linked networks are 700 and 580 nm, 1 and 6, and 3400 and  $\leq 3900$  cm $^{-1}$ , respectively. The spectra in Figure 9 show a smooth and gradual change in the emission spectra. As the conversion increases, more intense blue-shifted emissions emerge. No emission from strongly cured networks is observed at conversions below 40%, whereas emission from pure monomer at high conversions cannot be excluded. From analysis of the shape and half-width of the emission spectra displayed in Figure 9, it is concluded that the luminophores are present in a broadening and expanding range of environments as the reaction proceeds.<sup>31</sup>

To correlate the emission of the luminophores with the structure of the networks, a detailed knowledge of the emission of **1–5** in various “intermediate” environments is required. Emission spectra of **1–5** in PMMA/MMA mixtures indicate that the presence of dissolved polymer molecules induces modest changes in the emission of the probe molecules. Upon addition of 40% PMMA, transforming a liquid of low viscosity into a very viscous polymer solution,  $\lambda_{\text{max}}$  of **1** has shifted from 691 to 677 nm and HW from 3250 to 3500 cm $^{-1}$ , while  $I_{\text{max}}$  has increased by a factor 1.5. It seems reasonable to expect a fairly constant emission of probe molecules in media where many monomer molecules are present. These might be pools of monomer surrounded by highly cross-linked regions but also lightly cross-linked regions that contain appreciable amounts of monomer. The inability of all probes to detect microgels at low conversions seems to indicate that these particles have a low cross-link density and contain monomer. The other end of the spectrum, close to the fully cured networks, is less explored. The effects of the cross-link density on the emission characteristics of the luminophore are not known. Another uncertain factor is the diameter of the surrounding medium that is being monitored by the probe. This might be relevant in cases where luminophores are encapsulated in small “microgel” particles.

## Conclusions

We have investigated the emission of a series of 4-(dialkylamino)-4'-nitrostilbene-based reactive and nonreactive fluorescent probes **1–5** in various dimethacrylates. From these studies conclusions concerning the practical advantages of employing reactive probes and the mechanism by which **1–5** monitor the photoinitiated polymerization of dimethacrylates are drawn.

For monitoring the photoinitiated polymerization of dimethacrylates reactive probes are more sensitive than nonreactive counterparts, in particular during the first stages of the polymerization reaction. As expected, the differences between the difunctional reactive and nonreactive probes **4** and **5** are larger than for the monofunctional probes **2** and **3**. Apart from the increased sensitivity, additional benefits of the reactive probes **2** and **4** over the “naked” luminophore **1** are blue-shifted emissions (by 15–30 nm) and increased quantum yield of fluorescence  $\Phi_f$  (by a factor 1.5–2).

The magnitude and development of the differences in  $\lambda_{\text{max}}$  and HW values are clear indications of the mechanism by which all probes monitor the photoinitiated polymerization of dimethacrylates. During the polymerization of multifunctional methacrylates inhomogeneous media are formed. Probe molecules are distributed over various environments ranging from monomer-rich mobile environments ( $\lambda_{\text{max}} = 700\text{--}650$  nm) to rigid



highly cross-linked regions ( $\lambda_{\max} = 560\text{--}590\text{ nm}$ ). The numerical distribution of luminophores over all environments determines the probe's emission. Nonreactive probes diffuse out of cross-linking regions, and therefore smaller blue shifts in  $\lambda_{\max}$  are observed, in particular at low conversions. The increased sensitivity of difunctional reactive probes compared to monofunctional reactive probes is explained by a faster incorporation in the network.

Current research is focused on systems comprised of monomethacrylates, dimethacrylates, and nonreactive diluents, which form polymers in which the cross-link density and the homogeneity of the photoformed networks can be modified in a (more) controlled fashion.

**Acknowledgment.** This research was funded by the Royal Netherlands Academy for Arts and Sciences (KNAW). The authors thank Dr. J. M. Warman and Ir. R. D. Abellon (IRI, Delft University of Technology) for helpful discussions and the use of experimental facilities.

## References and Notes

- (1) Kloosterboer, J. G. *Adv. Polym. Sci.* **1988**, *84*, 1.
- (2) *Radiation Curing Science and Technology*; Pappas, S. P., Ed.; Plenum Press: New York, 1992.
- (3) (a) Chiu, Y. Y.; Lee, L. J. *J. Polym. Sci., Part A: Polym. Chem.* **1995**, *33*, 257. (b) Chiu, Y. Y.; Lee, L. J. *J. Polym. Sci., Part A: Polym. Chem.* **1995**, *33*, 269.
- (4) Anseth, K. S.; Bowman, C. N. *J. Polym. Sci., Part B: Polym. Phys.* **1995**, *33*, 1769.
- (5) Kloosterboer, J. G.; van de Hei, G. M. M.; Boots, H. M. J. *Polymer* **1984**, *25*, 354.
- (6) Microgels are regions that have above average conversion and cross-link density, which are localized around a center of initiation.
- (7) Consumption of pendant double bonds results in an increase of cross-link density or the formation of cycles in the main chain.
- (8) This statement is valid only, if the ratio between cycle and cross-link formation is constant during this stage of the reaction.
- (9) Rabek, J. F. In *Radiation Curing in Polymer Science and Technology*; Fouassier, J. P.; Rabek, J. F., Eds.; Elsevier Applied Science: London, 1993; Vol. 1.
- (10) (a) Decker, C.; Moussa, K. *Macromolecules* **1989**, *22*, 4455. (b) Dietz, J. E.; Elliot, B. J.; Peppas, N. A. *Macromolecules* **1995**, *28*, 5163.
- (11) (a) Clark, S. C.; Hoyle, C. E.; Jonsson, S.; Morel, F.; Decker, C. *Polymer* **1999**, *40*, 5063. (b) Anseth, K. S.; Rothenberg, M. D.; Bowman, C. N. *Macromolecules* **1994**, *27*, 2890. (c) Dickinson, P. R.; Sung, C. S. P. *Macromolecules* **1992**, *25*, 3758.
- (12) (a) Tyson, G. R.; Schultz, A. R. *J. Polym. Sci., Part A: Polym. Chem.* **1979**, *17*, 2059. (b) Kloosterboer, J. G.; Van de Hei, G. M. M.; Boots, H. M. J. *Polymer* **1984**, *25*, 354. (c) Cook, W. D. *Polymer* **1992**, *33*, 2152.
- (13) (a) Kim, Y. S.; Sung, C. S. P. *J. Appl. Polym. Sci.* **1995**, *57*, 363. (b) Pyun, E.; Sung, C. S. P. *Macromolecules* **1991**, *24*, 855.
- (14) Hu, S.; Polpielarz, R.; Neckers, D. C. *Macromolecules* **1998**, *31*, 4107. (b) Paczkowski, J.; Neckers, D. C. *Macromolecules* **1992**, *25*, 548.
- (15) (a) Wang, F. W.; Lowry, R. E.; Grant, W. H. *Polymer* **1984**, *25*, 690. (b) Valdez-Aguilera, O.; Pathak, C. P.; Neckers, D. C. *Macromolecules* **1990**, *23*, 689.
- (16) (a) Jager, W. F.; Volkers, A. A.; Neckers, D. C. *Macromolecules* **1995**, *28*, 8153. (b) Schaeken, T. C.; Warman, J. M. *J. Phys. Chem.* **1995**, *99*, 6145.
- (17) (a) Rettig, W. *Angew. Chem., Int. Ed. Engl.* **1986**, *25*, 971. (b) Paczkowski, J.; Neckers, D. C. *Macromolecules* **1991**, *24*, 3013.
- (18) (a) Jager, W. F.; Kudasheva, D.; Neckers, D. C. *Macromolecules* **1996**, *29*, 7351. (b) Wróblewski, S.; Trzebiatowska, K.; Jedrzejewska, B.; Pietrzak, M.; Gawinecki, R.; Paczkowski, J. *J. Chem. Soc., Perkin Trans. 2* **1999**, 1909. (c) Strehmel, B.; Strehmel, V.; Younes, M. *J. Polym. Sci., Part B: Polym. Phys.* **1999**, *37*, 1367.
- (19) For ICT probes like **1**, large differences in dipole moment between the ground state and the fluorescent excited state are observed. Therefore, the emission of this probe is sensitive to the polarity and the mobility of "solvent" molecules in the direct vicinity of the probe; see refs 16b and 16a.
- (20) This process closely resembles to photodiffusion, where more reactive species are enriched in initially polymerized regions. See: Broer, D. J.; Mol, G. N.; van Haaren, J. A. M. M.; Lub, J. *Adv. Mater.* **1999**, *11*, 573. (b) van Nostrum, C. F.; Nolte, R. J. M.; Broer, D. J. *Chem. Mater.* **1998**, *10*, 135.
- (21) Reactive fluorescent probes have been employed for monitoring polymerization processes. See: (a) Warman, J. M.; Abellon, R. D.; Verheij, H. J.; Verhoeven, J. W.; Hofstra, J. W. *J. Phys. Chem. B* **1997**, *101*, 4913. (b) Phelan, J. C.; Sung, C. S. P. *Macromolecules* **1997**, *30*, 6845.
- (22) Li, W.-H.; Hamielec, A. E.; Crowe, C. M. *Polymer* **1989**, *30*, 1513.
- (23) Jager, W. F.; Sarker, A. M.; Neckers, D. C. *Macromolecules* **1999**, *32*, 8791.
- (24) **P2** is the copolymer obtained from a random copolymerization of **2** with 100 equiv of MMA; see ref 23.
- (25) The sensitivity is the blue shift in emission wavelength  $\lambda_{\max}$  after full polymerization.
- (26) Bleaching of the probe occurs due to addition of the initiator radicals to the probe.
- (27) Covalent attachment to the polymer backbone leads to increases in fluorescence quantum yields  $\Phi_f$  as well, but these increases are limited to an estimated 10–15% in solution.
- (28) These mechanisms are complementary and represent extreme cases. Both mechanisms are expected to be valid.
- (29) This value is based on the polymerization of MMA; see ref 23.
- (30) Formulations with [probe] =  $1.0 \times 10^{-2}$  mol kg<sup>-1</sup> were employed since the extent photobleaching is limited, especially at the lower conversions.
- (31) At higher conversions, above 70% conversion, the range of environments in which the probe molecules reside decreases, as is illustrated by Figure 6.

MA0007278